ROBUST CONTROLLER DESIGN FOR IMPROVING VEHICLE ROLL CONTROL

H. DU* and N. ZHANG

Mechatronics and Intelligent Systems, Faculty of Engineering, University of Technology, Sydney,
P. O. Box 123, Broadway, NSW 2007, Australia

ABSTRACT–This paper presents a robust controller design approach for improving vehicle dynamic roll motion performance and guaranteeing the closed-loop system stability in spite of vehile parameter variations resulting from aging elements, loading patterns, and driving conditions, etc. The designed controller is linear parameter-varying (LPV) in terms of the time-varying parameters; its control objective is to minimise the H_∞ performance from the steering input to the roll angle while satisfying the closed-loop pole placement constraint such that the optimal dynamic roll motion performance is achieved and robust stability is guaranteed. The sufficient conditions for designing such a controller are given as a finite number of linear matrix inequalities (LMIs). Numerical simulation using the three-degree-of-freedom (3-DOF) yaw-roll vehicle model is presented. It shows that the designed controller can effectively improve the vehicle dynamic roll angle response during J-turn or fishhook maneuver when the vehicle's forward velocity and the roll stiffness are varied significantly.

KEY WORDS : Vehicle, Rollover, Active roll control, Linear parameter-varying, Pole placement

1. INTRODUCTION

Vehicle rollover incidences are a worldwide public safety issue and prevention of rollover crashes is crucial for safe highway operations. On the one hand, rollover prevention can be achieved by employing a rollover warning system (Chen and Peng, 2001), which requires the development of rollover criteria (Kim et al., 2006). On the other hand, an active roll control (ARC) system needs to be developed to assist the driver in actively preventing rollover accidents. Currently, the use of active roll control systems to improve vehicle roll stability and to reduce the likelihood of rollover accidents has been proposed and developed for heavy road vehicles (Sampson and Cebon, 2003; Miege and Cebon, 2005a; Miege and Cebon, 2005b).

Since commercial vehicles always operate in highly variable environments, parameter variations resulting from aging elements, loading patterns, and driving conditions, etc., will be unavoidable and these variations will considerably influence the vehicle dynamics. Hence, it is required that the designed ARC system should be robust and stable with regard to the variations of the vehicle parameters within reasonable bounds and should also retain good performance in spite of the parameter vari-

ations. For a heavy vehicle with time-variable forward velocity, a customary linear interpolation method was used to obtain the interpolated control law between the fixed speed controllers (Miege and Cebon, 2005a). At the same time, a gain-scheduled controller and linear parameter-varying (LPV) controller have been developed in Kim and Park (2004) and Gaspar et al. (2005), respectively, to deal with the variations of vehicle dynamics, assuming real-time measurement of varying forward speed was available. In fact, except for the varied vehicle forward velocity, there are many other parameters such as roll stiffness, centre of gravity (CG), and track width, etc., affecting the roll stability of the vehicles (Jang and Marimuthu, 2006; Takano et al., 2003) directly. Dealing with these parameter uncertainties in the controller design process becomes essential in real-world applications.

In this paper, an optimal robust LPV H_∞ controller that considers the closed-loop pole placement constraint is designed for a three-degree-of-freedom (3-DOF) yaw-roll vehicle model, with the goals of retaining the dynamic roll motion performance and providing robust stability subject to the parameter variations. Sufficient conditions for designing such a controller are given in terms of a finite number of linear matrix inequalities (LMIs). Simulation results show that despite the variations in parameters, such as vehicle forward velocity and roll stiffness, the designed parameter-dependent state feedback

---

*Corresponding author. e-mail: hdu@eng.uts.edu.au

controller is capable of achieving good roll control performance and robust stability.

The subsequent parts of this paper are organised as follows. Section 2 presents the description of a 3-DOF yaw-roll model under study. The formulation of an LPV H_∞ control problem and the conditions for designing such a controller are given in Section 3. Section 4 presents the simulation results. Finally, we conclude our findings in Section 5.

2. VEHICLE DYNAMICS MODEL

In developing the controller for active roll control of vehicles, it is not desirable to use the nonlinear complex vehicle models due to the difficulty of implementing the control system in real-world applications. Hence, in this paper, a 3-DOF yaw-roll model is used for the design of the controller. Vehicle parameters for a 1997 Jeep Cherokee published in (Chen and Peng, 2001) are used to construct the 3-DOF model based on Lagrangian dynamics. A view of the 3-DOF yaw-roll model is shown in Figure 1.

After including the direct roll moment as one of the control inputs, the equations of motion in matrix form for the 3DOF yaw-roll model are given as

$$
\begin{bmatrix} M & 0 & M_s h & 0 \\ 0 & I_z & I_{xz} & 0 \\ Mh & I_{xz} & I_x & 0 \\ 0 & 0 & 0 & 1 \end{bmatrix} \begin{bmatrix} \dot{v} \\ \dot{r} \\ \dot{p} \\ \dot{\phi} \end{bmatrix} + \begin{bmatrix} -\dfrac{Y_\beta}{u_0} & Mu_0 - Y_r & 0 & -Y_\phi \\ -\dfrac{N_\beta}{u_0} & -N_r & 0 & -N_\phi \\ 0 & M_s h u_0 & -L_p & -L_\phi \\ 0 & 0 & -1 & 0 \end{bmatrix} \begin{bmatrix} v \\ r \\ p \\ \phi \end{bmatrix}
$$

$$
= \begin{bmatrix} Y_\delta \\ N_\delta \\ 0 \\ 0 \end{bmatrix} \delta_{tire} + \begin{bmatrix} 0 \\ 0 \\ 1 \\ 0 \end{bmatrix} M_z ,
$$

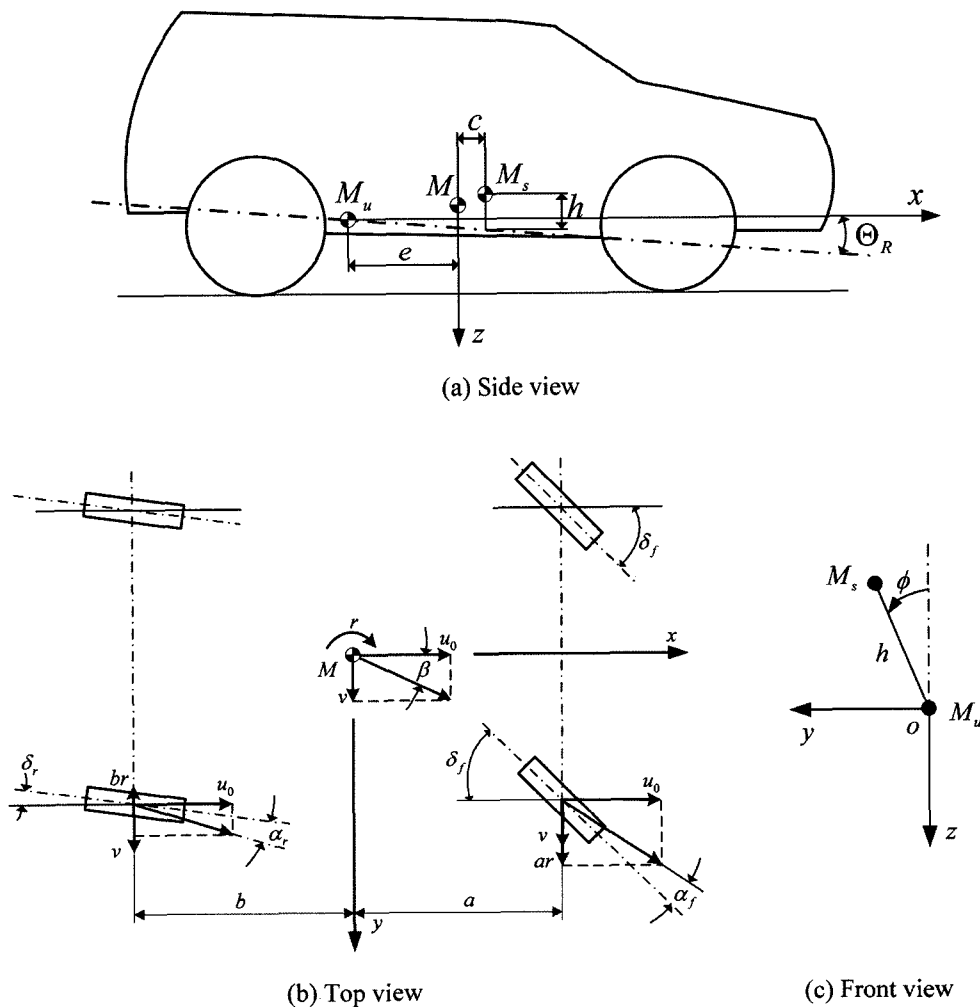where v is the lateral velocity, r is the yaw rate, p is the

(a) Side view

(b) Top view

(c) Front view

Figure 1. 3-DOF yaw-roll model.

roll rate, ϕ is the roll angle of the sprung mass, δ_{tire} is the steering input, and M_Z is the roll moment. In the matrices, u_0 is the vehicle forward velocity, M_s is the sprung mass, h is the distance from the centre of gravity of sprung mass to the roll axis, $L_\phi=M_sgh-K_R$, and $L_p=-c_R$ where K_R and c_R are roll stiffness and roll damping coefficient, respectively. Detailed descriptions of other entries in Equation (1) can be found in the Appendix.

If we define the state vector as $x=[v\ r\ p\ \phi]^T$ the state-space form of Equation (1) is expressed as

$$\dot{x} = Ax + B_1 w + B_2 u, \tag{2}$$

$$\text{where } A = -\begin{bmatrix} M & 0 & M_s h & 0 \\ 0 & I_z & I_{xz} & 0 \\ Mh & I_{xz} & I_x & 0 \\ 0 & 0 & 0 & 1 \end{bmatrix}^{-1} \begin{bmatrix} -\dfrac{Y_\beta}{u_0} & Mu_0-Y_r & 0 & -Y_\phi \\ -\dfrac{N_\beta}{u_0} & -N_r & 0 & -N_\phi \\ 0 & M_s h u_0 & -L_p & -L_\phi \\ 0 & 0 & -1 & 0 \end{bmatrix},$$

$$B_1 = \begin{bmatrix} M & 0 & M_s h & 0 \\ 0 & I_z & I_{xz} & 0 \\ Mh & I_{xz} & I_x & 0 \\ 0 & 0 & 0 & 1 \end{bmatrix}^{-1} \begin{bmatrix} Y_\delta \\ N_\delta \\ 0 \\ 0 \end{bmatrix}, \quad B_2 = \begin{bmatrix} M & 0 & M_s h & 0 \\ 0 & I_z & I_{xz} & 0 \\ Mh & I_{xz} & I_x & 0 \\ 0 & 0 & 0 & 1 \end{bmatrix}^{-1} \begin{bmatrix} 0 \\ 0 \\ 1 \\ 0 \end{bmatrix},$$

$w=\delta_{tire}$ is steering disturbance (the steering input is viewed as the disturbance to the system), and $u=M_z$ is the control input. Although this model is obtained under the constant vehicle velocity assumption, validation against experimental data (Chen and Peng, 2001) shows that this model is still acceptable even when the vehicle forward velocity is varied.

3. OPTIMAL LPV H∞ CONTROLLER DESIGN

3.1. H∞ Performance

When the time-varying parameters are considered in Model (2), the vehicle model becomes an LPV model and this LPV model is expressed as

$$\dot{x}=A(p)x+B_1(p)w+B_2(p)u, \tag{3}$$

where the matrices $A(p)$, $B_1(p)$, and $B_2(p)$ are continuous functions of p which is a time-varying parameter vector and can be measured in real-time. Assume matrices $A(p)$, $B_1(p)$, and $B_2(p)$ are constrained to the polytope P given by

$$P = \left\{ (A,B_1,B_2)(p): (A,B_1,B_2)(p) = \sum_{i=1}^{N} \rho_i(p)(A,B_1,B_2)_i, \right.$$

$$\left. \sum_{i=1}^{N} \rho_i(p) = 1, \ \rho_i(p) \geq 0, \ i=1,...,N \right\}. \tag{4}$$

It is clear that the knowledge of the value of ρ_i defines a precisely known system inside the polytope P described by the convex combination of its N vertices. Although ρ_i

does not necessarily represent the actual time-varying parameter p of the dynamical system, there exists a linear relationship between p and ρ_i that can be easily determined from the physical model whenever p affinely affects the linear system. For example, if there are three time-varying parameters p_1, p_2, and p_3 in the model, and the eight vertices of the polytope P are defined as

$$V_1: =[p_{1min}\ p_{2min}\ p_{3min}], \quad V_2: =[p_{1max}\ p_{2min}\ p_{3min}],$$

$$V_3: =[p_{1min}\ p_{2max}\ p_{3min}], \quad V_4: =[p_{1max}\ p_{2max}\ p_{3min}],$$

$$V_5: =[p_{1min}\ p_{2min}\ p_{3max}], \quad V_6: =[p_{1max}\ p_{2min}\ p_{3max}], \tag{5}$$

$$V_7: =[p_{1min}\ p_{2max}\ p_{3max}], \quad V_8: =[p_{1max}\ p_{2max}\ p_{3max}],$$

where p_{imin} and p_{imax}, $i=1, 2, 3$, denote the minimum value and the maximum value of parameter p_i, respectively, then the convex coordinates ρ_i, $i=1, 2,..., 8$, can be given as

$$\rho_1 = \zeta\xi\delta, \rho_2 = (1-\zeta)\xi\delta, \rho_3 = \zeta(1-\xi)\delta, \rho_4 = (1-\zeta)(1-\xi)\delta,$$

$$\rho_5 = \zeta\xi(1-\delta), \rho_6 = (1-\zeta)\xi(1-\delta), \rho_7 = \zeta(1-\xi)(1-\delta), \tag{6}$$

$$\rho_8 = (1-\zeta)(1-\xi)(1-\delta),$$

where

$$\zeta = \frac{p_{1max}-p_1}{p_{1max}-p_{1min}}, \xi = \frac{p_{2max}-p_2}{p_{2max}-p_{2min}}, \delta = \frac{p_{3max}-p_3}{p_{3max}-p_{3min}}, \tag{7}$$

and therefore, the varying-parameter model can be expressed as

$$(A,B_1,B_2)(p)= \sum_{i=1}^{8} \rho_i(p)(A,B_1,B_2)_i, \tag{8}$$

where the vertex matrices $(A, B_1, B_2)_i$, $i=1, 2,.., 8$, are obtained by replacing the values of p_1, p_2, and p_3 in the model with those values defined in V_1, V_2,..., and V_8, respectively.

To design a controller for an active roll control system, one should indicate the control output, which is the variable of interest that needs to be controlled so that the performance index from the disturbance input to the control output can be realised with the specified requirement. For system (3), we indicate the control output as

$$z=C_1 x+D_{12}w+D_{12}u, \tag{9}$$

where C_1, C_{11}, C_{12} are problem-dependent constant matrices. For example, if we want the roll angle to be controlled, we can choose $C_1=[0\ 0\ 0\ 1]$, $D_{11}=0$, $D_{12}=0$; if we want the control moment to be constrained (e.g., we hope that the amplitude of the control moment or the consumed power of the control moment should be less than a given level), we can choose $C_1=0$, $D_{11}=0$, and $D_{12}=I$ to define the control output.

In this paper, we are interested in designing a state feedback parameter-dependent controller

$$u = K(p)x = \sum_{i=1}^{N} \rho_i(p)K_i x, \quad \sum_{i=1}^{N} \rho_i(p) = 1, \rho_i(p) \geq 0, \quad (10)$$

$$i = 1, \ldots, N$$

for system

$$\dot{x} = A(p)x + B_1(p)w + B_2(p)u,$$
$$z = C_1 x + D_{11}w + D_{12}u, \quad (11)$$

such that the closed-loop system is stable and the H_∞ performance $\|T_{zw}\|_\infty$ is minimised, where T_{zw} is the closed-loop transfer function from the disturbance w to the control output z.

3.2. Pole Placement Requirement

Generally, H_∞ performance design does not directly deal with the transient response of the closed-loop system. Therefore, in addition to the H_∞ performance mentioned above, to obtain the satisfied dynamic performance, we also require the closed-loop poles are to be placed in the region $S(\alpha, r, \theta)$ as defined in Figure 2. In many practical applications, exact pole assignment may not be necessary. It is sufficient to locate the closed-loop poles in a prescribed subregion in the complex left half plane. By confining the closed-loop poles to the region $S(\alpha, r, \theta)$, we can ensure a minimum decay rate α, a minimum damping ratio $\zeta(=r\cos\theta)$, and a maximum damped natural frequency ω_d $(=r\sin\theta)$ for the closed-loop system. These, in turn, bound the maximum overshoot, the frequency of oscillation, the decay time, the rise time, and the settling time for the closed-loop system transient response.
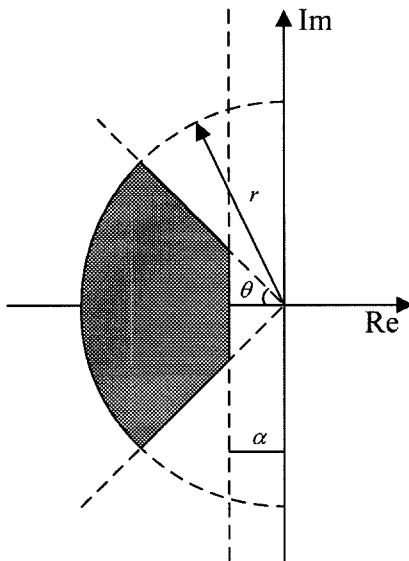

Figure 2. The system pole placement region $S(\alpha, r, \theta)$.

3.3. Formulation for the Controller Synthesis

For simplicity, we only consider the case in which the time-varying parameter p does not affect the matrices B_1 and B_2. In such a case, the synthesis of the state feedback controller that guarantees the optimal H_∞ performance and satisfies the additional constraint on the closed-loop pole locations can be achieved based on the sufficient conditions provided in the following theorem.

Theorem 1 Minimise γ over positive symmetric matrix X and matrix Y_i, subject to the following LMI constraints:

$$\begin{bmatrix} A_i X + XA_i^T + B_2 Y_i + Y_i^T B_2^T & B_1 & XC_1^T + Y_i^T D_{12}^T \\ * & -\gamma & D_{11}^T \\ * & * & -\gamma \end{bmatrix} < 0, \quad (12)$$

$$A_i X + XA_i^T + B_2 Y_i + Y_i^T B_2^T + 2\alpha X < 0, \quad (13)$$

$$\begin{bmatrix} -rX & A_i X + B_2 Y_i \\ * & -rX \end{bmatrix} < 0, \quad (14)$$

$$\begin{bmatrix} \sin\theta \left[A_i X + B_2 Y_i + XA_i^T + (B_2 Y_i)^T \right] \\ * \end{bmatrix}$$
$$\begin{bmatrix} \cos\theta \left[A_i X + B_2 Y_i - XA_i^T - (B_2 Y_i)^T \right] \\ \sin\theta \left[A_i X + B_2 Y_i + XA_i^T + (B_2 Y_i)^T \right] \end{bmatrix} < 0, \quad (15)$$

$$i = 1, 2, \ldots, N,$$

where the notation $*$ is used to represent a block matrix which is readily inferred by symmetry.

Given a solution (X, Y_i) of this minimisation problem, the optimal H_∞ state feedback control gain is obtained as $K_i = Y_i X^{-1}$ and the LPV controller is synthesised as

$$K(p) = \sum_{i=1}^{N} \rho_i(p)K_i$$

The proof of Theorem 1 can be easily derived following a similar procedure from (Montagner et al., 2005; Chilali and Gahinet, 1996), of which details are omitted here for brevity. If the time-varying parameter p also affect the matrices B_1 and B_2 as shown in Equation (3), the sufficient conditions will be relatively complicated but can still be derived using a similar procedure which is not provided in this paper.

4. SIMULATION RESULTS

In this section, we will apply the proposed approach to design the optimal LPV H_∞ controller based on the 3-DOF yaw-roll model described in Section 2. The parameters of the 3-DOF 1997 Jeep Cherokee yaw-roll model selected for this study are listed in Appendix. In this study, simulations are conducted using software MATLAB/ Simulink.

Assume that all the state variables defined in Equation (2) are measurements available for feedback, that is, we

can design a full-state feedback controller. As an example, we consider the vehicle forward velocity u_0 and the roll stiffness K_R as the time-varying parameters, and define the time-varying parameter vector p as 36 km/h $\leq$ $p_1=u_0 \leq 180$ km/h, $p_2=1/u_0$, and $p_3=K_R$, where the roll stiffness K_R is varied within 20% of its nominal value for designing the LPV controller. The design objective is to minimise the effect of disturbance w on the roll angle by minimising $\|T_{zw}\|_\infty$ and to constrain the closed-loop poles in the indicated region $S(0, 20, \pi/3)$ Using the approach presented in Section 3, we obtain such an LPV controller as defined in (10). For description in brevity, we denote this designed controller as Controller I hereafter.

To evaluate the performance of the designed controller in the time domain, two kinds of maneuvers are used: one is J-turn maneuver in which the steering input angle is defined as that in Kim and Park (2004), and the other is a fishhook maneuver which is similar to that presented in Jang and Marimuthu (2006) but with different definitions for the steering amplitude and time range.

During the J-turn maneuver, the responses of the roll angle for both the passive and the active control systems are plotted in Figure 3 for different vehicle forward velocities. The forward velocity is increased from 36 km/h to 180 km/h, and the other parameters are kept as nominal values which are given in Appendix. It can be seen from Figure 3 that the roll angle response for the passive system ($u=0$) varies largely with the variation of forward velocity during the J-turn maneuver, but on the contrary, the roll angle response of the active system which is realised by Controller I is maintained throughout in spite of the variation of the forward velocity. In particular, the transient processes are all very smooth and the

Figure 4. Yaw rate response during J-turn maneuver at different vehicle forward velocities. Vehicle forward velocity increases from 36 km/h to 180 km/h with step 36 km/h.

overshoot values are all close to the steady-state values.

Figure 4 shows yaw rate response with respect to the varied forward velocity. It can be seen that although the yaw rate is varied significantly with the variation of forward velocity, there is no great difference between the passive system and the active system for yaw rate at a given forward velocity. This means that the proposed control approach has little effect on the yaw motion. Similarly, we change the roll stiffness to different values but keep the forward velocity at 72 km/h and the other parameters as nominal values in order to see the dynamic performances realised by the two systems.

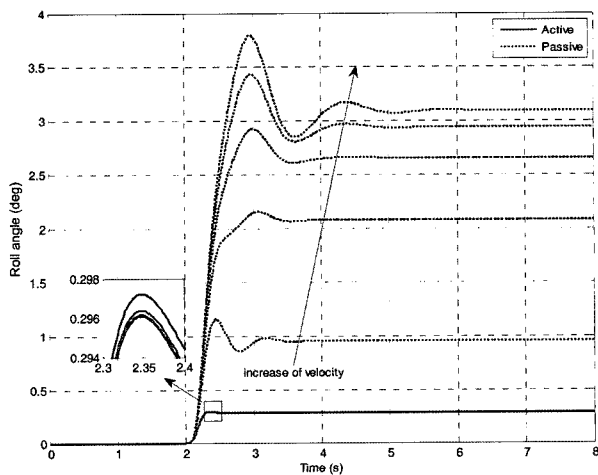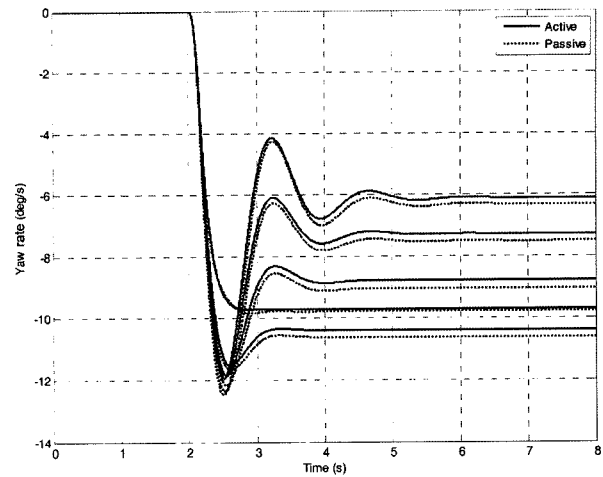Figure 5 shows the roll angle responses for the two

Figure 3. Roll angle response during J-turn maneuver at different vehicle forward velocities. Vehicle forward velocity increases from 36 km/h to 180 km/h with step 36 km/h.
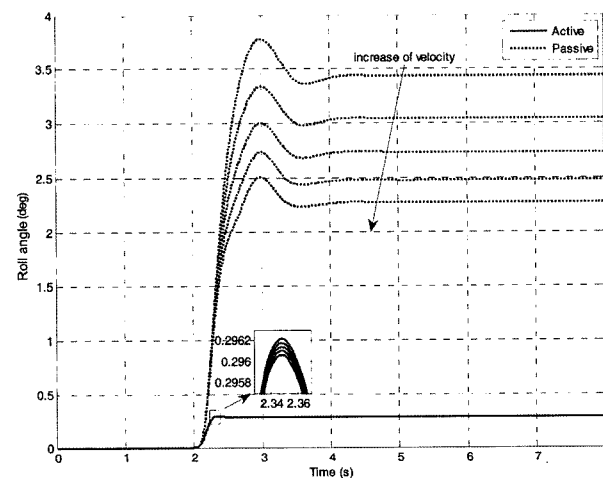

Figure 5. Roll angle response during J-turn maneuver at different roll stiffnesses. Roll stiffness increases from 45566 Nm/rad to 65566 Nm/rad with step 5000 Nm/rad.
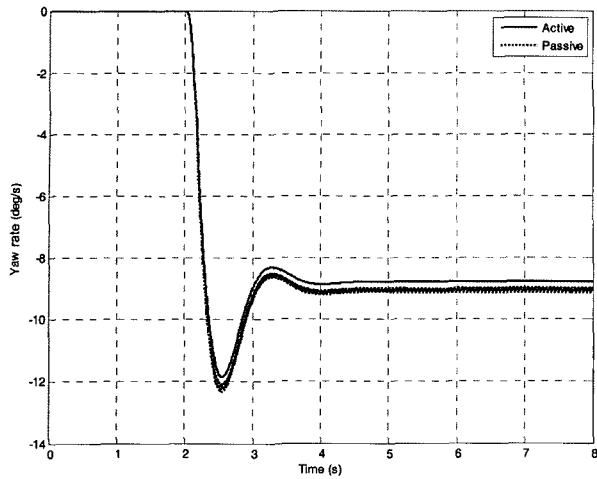
Figure 6. Yaw rate response during J-turn maneuver at different roll stiffnesses. Roll stiffness increases from 45566 Nm/rad to 65566 Nm/rad with step 5000 Nm/rad.

systems with different roll stiffnesses which are varied from about −20% to 20% of its nominal value. It can be seen that roll stiffness significantly affects the roll performance of the passive system as analysed in Takano et al. (2003). However, with the designed control system, the dynamic roll performance is least affected by the variation of the roll stiffness.

Figure 6 shows the yaw rate response with respect to the variation of roll stiffness. It can be seen that the variation of roll stiffness does not affect the yaw motion. Additionally, there is little difference between the passive system and the active system for the yaw rate response with any given roll stiffness.
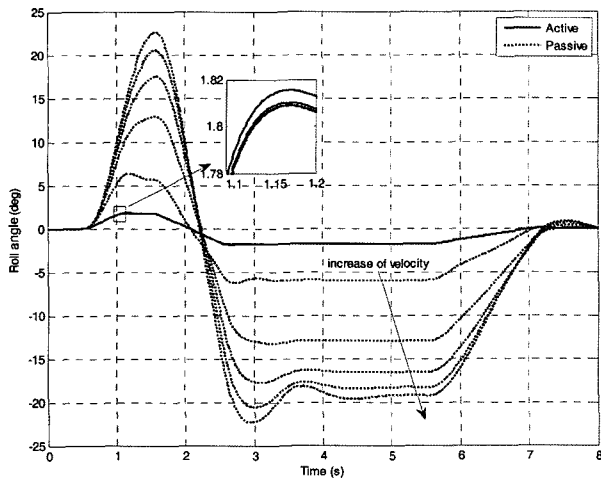

Figure 7. Roll angle response during fishhook maneuver at different vehicle forward velocities. Vehicle forward velocity increases from 36 km/h to 180 km/h with step 36 km/h.
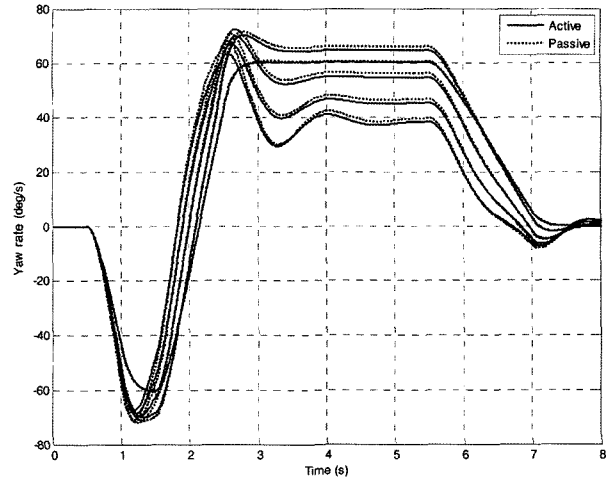

Figure 8. Yaw rate response during fishhook maneuver at different vehicle forward velocities. Vehicle forward velocity increases from 36 km/h to 180 km/h with step 36 km/h.

During the fishhook maneuver, the roll angle responses for the passive and active systems at different velocities and different roll stiffnesses are plotted in Figures 7 and 9, respectively. It can be seen from these two figures that the designed controller can retain good performance regardless of the variations in the forward velocity and roll stiffness while a different maneuver is applied. The yaw rate responses for the passive and active systems at different velocities and different roll stiffnesses are plotted in Figures 8 and 10, respectively. It can be seen from these two figures that the designed controller has little effect on the yaw motion as compared to the passive system regardless of the variations in the
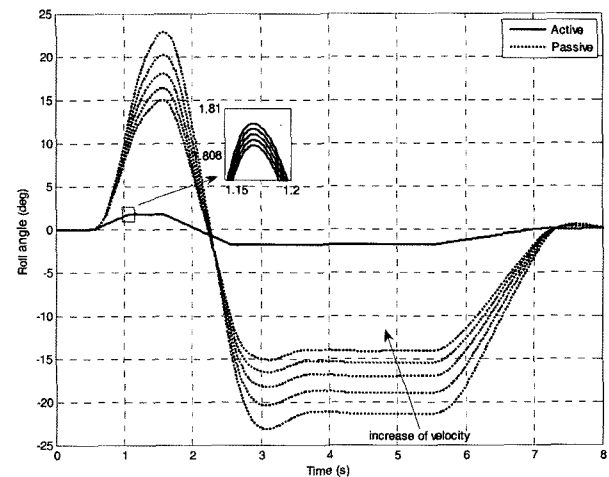

Figure 9. Roll angle response during fishhook maneuver at different roll stiffnesses. Roll stiffness increases from 45566 Nm/rad to 65566 Nm/rad with step 5000 Nm/rad.
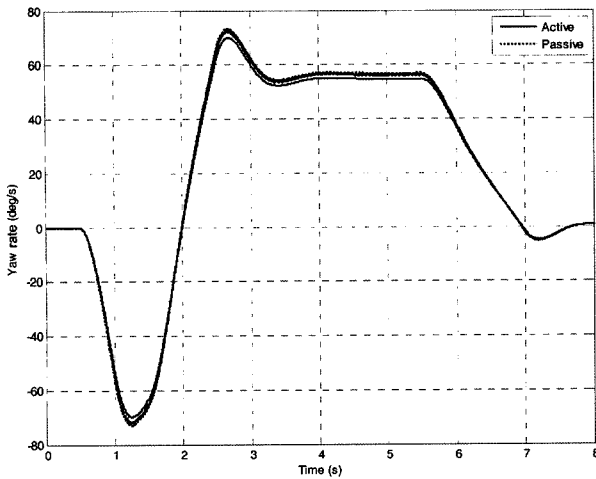
Figure 10. Yaw rate response during fishhook maneuver at different roll stiffnesses. Roll stiffness increases from 45566 Nm/rad to 65566 Nm/rad with step 5000 Nm/rad.
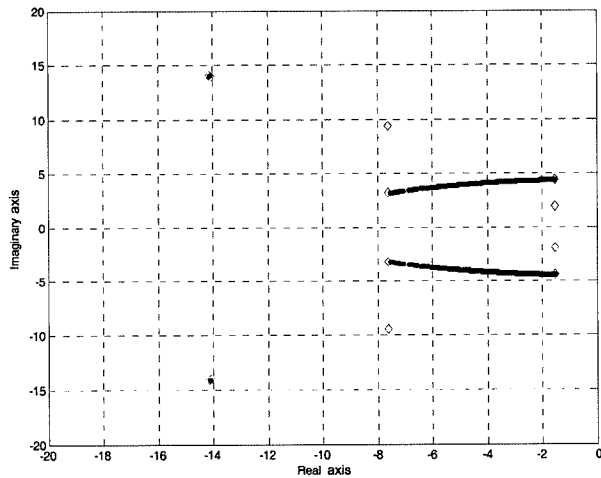

Figure 11. The closed-loop system poles for randomly generated forward velocity and roll stiffness. The poles of the closed-loop system vertices are represented by the diamond symbol.

forward velocity and roll stiffness with a different maneuver applied.

To further validate the closed-loop system performance and stability when the forward velocity and roll stiffness are varied, the closed-loop system poles for 500 randomly generated forward velocities and roll stiffnesses, within their respective ranges, are plotted in Figure 11. It can be seen from this figure that all of the closed-loop system poles are concentrated in several areas which all locate in the designed region $S(0, 20, \pi/3)$. This guarantees the dynamic response performance and the closed-loop system stability.

In addition, to show the advantages of the designed LPV controller, two more controllers are designed for comparison purposes based on the similar conditions presented in Section 3. One controller considers the variations in forward velocity and roll stiffness, but it is not parameter-dependent, i.e., the controller gain is fixed. This controller can be obtained by setting $Y_1=Y_2=\cdots=Y$ in Equations (12)~(15). After finding the matrices X and Y by resolving the LMIs in Equations (12)~(15), the obtained controller is given as $K=YX^{-1}$. For brevity, we denote this designed controller as Controller II hereafter. Another controller is designed for forward velocity 108 km/h and the nominal values for the roll stiffness and other parameters; that is, this controller does not consider variations in the forward velocity and roll stiffness. This controller can be easily obtained by solving the LMIs (12)~(15) with $N=1$. We denote this controller as Controller III for brevity.

In order to show the time domain performance of the closed-loop system composed by the three controllers, the same J-turn maneuver is applied with randomly generated forward velocity and roll stiffness. As examples, four cases are listed in Table 1, where the first row indicates the randomly generated forward velocity and roll stiffness; in the bracket, the first value is for the forward velocity in km/h, and the second value is for the roll stiffness in Nm/rad. The second row indicates the particular system, where 'O' means the passive system, 'I-III' mean the active systems which are composed by controllers I-III, respectively. 'ϕ_m' means the maximum roll angle in deg, 'ϕ_s' means the steady state roll angle in deg, 'M_m' means the maximum input moment in kN.m, 'M_s' means the input moment in steady-state in kN.m.

Table 1. Controller performance comparision for randomly generated forward speed and roll stiffness.

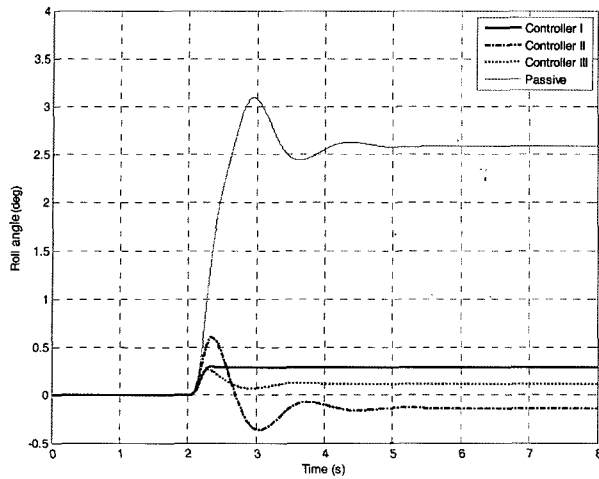| P	[161,65433]				[101,53546]				[83,67890]				[41,60787]			
C	O	I	II	III	O	I	II	III	O	I	II	III	O	I	II	III
ϕ_m	3.09	0.30	0.60	0.27	2.99	0.30	0.81	0.31	2.00	0.30	0.81	0.32	1.29	0.30	0.84	0.26
ϕ_s	2.59	0.29	0.14	0.12	2.76	0.29	0.55	0.31	1.89	0.29	0.69	0.32	1.08	0.29	0.84	0.26
M_m	0	2.77	3.37	2.99	0	2.18	1.95	2.16	0	1.80	1.36	1.76	0	0.76	0.42	0.79
M_s	0	2.35	2.78	2.53	0	2.03	1.81	2.01	0	1.72	1.29	1.69	0	0.76	0.23	0.78

Figure 12: Roll angle response during J-turn maneuver for different controllers with u_0=161 km/h, and K_R= 65433 Nm/rad.

Figure 13. Required moment for different controllers during J-turn maneuver.

For clarity, the dynamic responses for the first case are also plotted in Figure 12 and Figure 13 for the roll angle and the input moment, respectively.

It can be seen from Table 1 and Figures 12 and 13 that no matter what kinds of parameters are used, Controller I can always keep the maximum roll angle and steady state roll angle at similar values, but on the contrary, Controller II varied the roll angle outputs greatly in different cases. However, Controller II can guarantee the stability of the closed-loop system regardless of the variations on the parameters because it is designed with consideration of these parameter variations. Controller III can achieve good performance comparable to that realised by Controller I, or even better in steady-state than that of Controller I in some cases; however, this controller cannot theoretically guarantee closed-loop system stability when the actual vehicle parameters are different from the designed parameters. In addition, the required input moment for Controller III is larger than that required by Controller I, which will consume more power and will possibly cause an actuator saturation problem. These findings confirm that Controller I can better realise the desired dynamic roll motion performance and robust stability with acceptable input moment as compared to the other two controllers.

It should be noted in this study that the roll moment is assumed as the control input to be implemented. In practice, the roll moment can be provided by using hydraulic actuating system together with anti-roll bar (Sampson and Cebon, 2003; Miege and Cebon, 2005a). To overcome the potential problems with a hydraulic system, such as complexity due to the large number of hydraulic elements including pump, relief valve, accumulator, control valve, oil tank, pipes, etc., leakage during
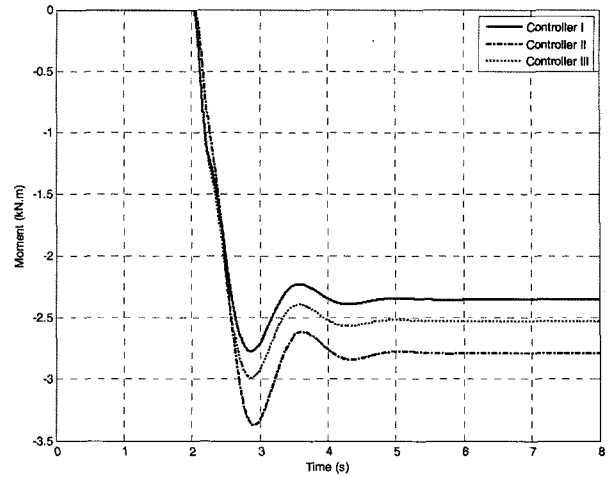
operation, and complicated maintenance, an electrically actuating system can be applied (Kim and Park, 2004).

5. CONCLUSIONS

This paper presents a robust controller design approach for vehicle roll motion control which considers variations in vehicle model parameters. By using the LMIs formulation, the required full-state feedback parameter-dependent controller can be obtained. A simulation example is used to demonstrate that the designed controller can effectively improve the dynamic roll motion performance when the vehicle parameters, such as forward speed and roll stiffness, change within reasonable magnitudes. This approach has the potential to incorporate more objectives, such as actuator saturation, actuator failure, etc., into the design process. Further work will be done to affinely express more key parameters in the matrices and to develop the effective online parameter identification algorithm.

REFERENCES

Chen, B. C. and Peng, H. (2001). Differential-braking-based rollover prevention for sport utility vehicles with human-in-the-loop evaluations. *Vehicle System Dynamics* **36**, 4, 359–389.

Chilali, M. and Gahinet, P. (1996). H_∞ design with pole placement constraints: An LMI approach. *IEEE Trans. Automatic Control* **41**, 3, 358–367.

Gaspar, P., Szaszi, I. and Bokor, J. (2005). Reconfigurable control structure to prevent the rollover of heavy vehicles. *Control Engineering Practice*, **13**, 699–711.

Jang, B. C. and Marimuthu, R. P. (2006). Sensitivity analysis of SUV parameters on rollover propensity. *Int. J. Automotive Technology* **7**, **6**, 703–714.

Kim, M. H., OH, J. H., Lee, J. H. and Jeon, M. C. (2006). Development of rollover criteria based on simple physical model of rollover event. *Int. J. Automotive Technology* **7**, **1**, 51–59.

Kim, H. J. and Park, Y. P. (2004). Investigation of robust roll motion control considering varying speed and actuator dynamics. *Mechatronics*, **14**, 35–54.

Miege, A. J. P. and Cebon, D. (2005a). Active roll control of an experimental articulated vehicle. *Proc. Instn. Mech. Engrs: Part D: J. Automobile Engineering*, **219**, 791–806.

Miege, A. J. P. and Cebon, D. (2005b). Optimal roll control of an articulated vehicle: Theory and model validation. *Vehicle System Dynamics* **43**, **12**, 867–893.

Montagner, V. F., Oliveira, R. C. L. F., Leite, V. J. S. and Peres, P. L. D. (2005). LMI approach for H_∞ linear parameter-varying state feedback control. *IEE Proc. Control Theory and Applications* **152**, **2**, 195–201.

Sampson, D. J. M. and Cebon, D. (2003). Active roll control of single unit heavy road vehicles. *Vehicle System Dynamics* **40**, **4**, 229–270.

Takano, S., Nagai, M., Taniguchi, T. and Hatano, T. (2003). Study on a vehicle dynamics model for improving roll stability. *JSAE Review*, **24**, 149–156.

APPENDIX

Detailed descriptions of entries in Equation (1):

$$M = M_s + M_u$$

$$Y_\beta = -(C_{af} + C_{ar})$$

$$Y_\phi = C_{ar}\frac{\partial \delta_r}{\partial \phi} + C_{yf}\frac{\partial \gamma_f}{\partial \phi}$$

$$Y_r = \frac{bC_{ar} - aC_{af}}{u_0}$$

$$Y_\delta = C_{af}$$

$$N_\beta = bC_{ar} - aC_{af}$$

$$N_r = -\frac{b^2 C_{ar} + a^2 C_{af}}{u_0}$$

$$N_\phi = aC_{yf}\frac{\partial \gamma_f}{\partial \phi} - bC_{ar}\frac{\partial \delta_r}{\partial \phi}$$

$$N_\delta = aC_{af}$$

$$I_x = (I_{xx})_s + M_s h^2 - 2\Theta_R(I_{xz})_s + \Theta_R^2(I_{zz})_s$$

$$I_{xz} = M_s hc - (I_{xz})_s + \Theta_R(I_{zz})_s$$

$$I_z = (I_{zz})_s + (I_{zz})_u + M_s c^2 + M_u e^2$$

Parameters used for a 1997 Jeep Cherokee

Symbol	Definition	Value	Unit
M_s	Rolling sprung mass	1663	kg
M_u	Non-rolling unsprung mass	325	KG
Θ_R	Inclination angle of the roll axis point down	0.0873	rad
a	Distance from the vehicle CG to the front axle	1.147	m
b	Distance from the vehicle CG to the rear axle	1.431	m
c	Distance from the CG of M_s to the vehicle CG	0.421	m
e	Distance from the CG of M_u to the vehicle CG	2.157	m
g	Gravity	9.81	m/s^2
h	Distance from the CG of M_s to the roll axis	0.306	m
C_{af}	Front tire cornering stiffness	59496	N/rad
C_{ar}	Rear tire cornering stiffness	109400	N/rad
$\partial \delta_r / \partial \phi$	Partial derivative of the roll induced steer at the rear axle	0.07	
$\partial \gamma_f / \partial \phi$	Partial derivative of the camber thrust at the front axle	0.8	
C_{yf}	Camber thrust coefficient at the front axle	2039	N/rad
K_R	Roll stiffness	56957	Nm/rad
c_R	Roll damping coefficient	3496	Nms/rad
$(I_{xx})_s$	Moment of inertia about the x-axis of the rolling sprung mass	602.8	kgm^2
$(I_{xz})_s$	Product of inertia about the x-z axes of the rolling sprung mass	90.0	kgm^2
$(I_{zz})_s$	Moment of inertia about the z-axis of the rolling sprung mass	2163.7	kgm^2
$(I_{zz})_u$	Moment of inertia about the z-axis of the non-rolling unsprung mass	540.0	kgm^2